

## Facile Synthesis and Structures of Cyclic Triimidazole and Its Boric Acid Adduct

David M. Schubert,\*† Daniel T. Natan,† Duane C. Wilson,† and Kenneth I. Hardcastle‡

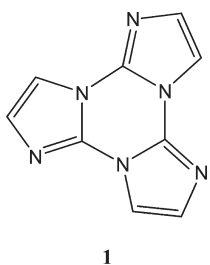
<sup>†</sup>U.S. Borax Inc, Rio Tinto Minerals, 8051 East Maplewood Avenue, Greenwood Village Colorado 80111, United States, and <sup>‡</sup>Crystallography Laboratory, Emory University, Atlanta, Georgia, United States

Received November 9, 2010; Revised Manuscript Received December 13, 2010

**ABSTRACT:** Cyclic triimidazole,  $C_9H_6N_6$  (**1**), was prepared by thermolysis of the easily prepared copper imidazolate framework solid,  $Cu(C_3H_3N_2)_2$  (**2**), providing a convenient route to this potentially useful tecton for molecular design. Anhydrous **1** and a hydrate, **1**· $0.5H_2O$ , were characterized by single-crystal X-ray diffraction. Hydrate **1**· $0.5H_2O$  contains two crystallographically independent **1** molecules. Supramolecular structures of **1** and **1**· $0.5H_2O$  feature stacking arrangements in which the **1** molecule deviates from idealized geometry. A 3-fold H-bond acceptor **1** forms an adduct with boric acid, **1**· $B(OH)_3$ , which was also structurally characterized. This adduct is composed of hydrogen-bonded sheets of **1** and  $B(OH)_3$  molecules with sheet interplanar separations of  $3.175(4)\text{ \AA}$  and  $B(OH)_3$  boron atoms positioned above and below the centroids of **1** in adjacent sheets. Unlike **1** and its hydrate, **1**· $B(OH)_3$  contains **1** molecules that display crystallographically required  $D_{3h}$  symmetry. Anhydrous **1** crystallizes in the triclinic system, space group  $P\bar{1}$ , with  $a = 7.2138(12)$ ,  $b = 8.3667(15)$ ,  $c = 8.8361(13)\text{ \AA}$ ,  $\alpha = 99.826(13)$ ,  $\beta = 113.825(10)$ ,  $\gamma = 110.721(11)^\circ$ ,  $V = 424.55(12)\text{ \AA}^3$ ,  $Z = 2$ ; **1**· $H_2O$  (or **1**· $0.5H_2O$ ), triclinic,  $P\bar{1}$ ,  $a = 7.5608(3)$ ,  $b = 7.5669(5)$ ,  $c = 15.8436(8)\text{ \AA}$ ,  $\alpha = 84.504(3)$ ,  $\beta = 81.269(3)$ ,  $\gamma = 87.038(3)^\circ$ ,  $V = 891.18(8)\text{ \AA}^3$ ,  $Z = 2$ ; **1**· $B(OH)_3$ , trigonal,  $P\bar{3}$ ,  $a = 10.1186(3)$ ,  $b = 10.1186(3)$ ,  $c = 6.3488(4)\text{ \AA}$ ,  $\alpha = 90^\circ$ ,  $\beta = 90^\circ$ ,  $\gamma = 120^\circ$ ,  $V = 562.94(4)\text{ \AA}^3$ ,  $Z = 2$ .

### Introduction

Cyclic triimidazole ( $C_9H_6N_6$ , **1**) is a useful tecton for molecular design.<sup>1</sup> This molecule is a 3-fold hydrogen bond acceptor, participates in molecular stacking interactions, and may be anticipated to form  $\sigma$ - and  $\pi$ -coordination compounds. These attributes make **1** a useful participant in supramolecular architectures and a potential template for the syntheses of other materials. Owing to its similarity to important biological compounds, **1** may also serve as a precursor to pharmaceutical and other biologically active substances. We found that **1** readily forms adducts with a variety of hydrogen bond donor compounds. As an example, **1** forms a 1:1 adduct with boric acid, **1**· $B(OH)_3$ . Here we describe a convenient synthesis method for **1** and single crystal X-ray structures of anhydrous **1**, as well as its hemihydrate and boric acid adduct.



### Experimental Section

**Materials and Methods.** Copper(II) oxide (<5  $\mu\text{m}$  particle size, 98%), 1-H-imidazole (99%), and acetic acid (99.8%) were obtained

from Sigma-Aldrich Chemical Co. and used without further purification. Silica gel was spherical type obtained from Fluka Analytical. Toluene (technical grade) and methylene chloride (HPLC grade) were used as received. Boric acid was produced by U.S. Borax Inc. Elemental analyses were carried out by Galbraith Laboratories, Knoxville, TN.

**Synthesis of Copper Imidazolate Precursor,  $Cu(C_3N_2H_3)_2$  (**2**).** Imidazole (138.89 g, 2.04 mol) was added to a hot stirred suspension of copper(II) oxide (79.44 g, 1.00 mol) in 2 L of 2% aqueous acetic acid. The mixture was heated at a boil for 1 h, during which time the mixture turned dark blue and thickened. Solid product was separated by filtration and washed with DI water until the filtrate was no longer blue. The solid product was dried at 105 °C, giving 105.0 g (53% yield) of blue polymorph of copper imidazolate, **2**. The powder X-ray diffraction (XRD) pattern of the product matched that reported in the literature and also showed the presence of a small amount of unreacted CuO.<sup>2</sup> As a substantial amount of copper remains in the dark blue filtrate, this solution was used as a solvent for subsequent batches, with addition of 2% aqueous acetic acid makeup solution, ultimately giving near quantitative yields of **2**.

**Synthesis of Cyclic Triimidazole (**1**).** A 300-mL round-bottom flask was charged with powdered  $Cu(C_3N_2H_3)_2$  (**2**, 49.42 g, 0.25 mol). A small plug of glass wool was placed in the neck of the flask, which was then fitted with a 20-cm long borosilicate glass tube and vacuum adapter using high temperature grease (Santovac 5GB Ultr). The assembly was mounted horizontally and evacuated slowly to avoid drawing **2** into the tube. The flask was heated with a surrounding heating mantle to 200 °C. The temperature was then slowly increased to 300 °C over ca. 3 h, during which time the crude organic product collected in the tube, and then maintained in vacuo for another 1 h at 300 °C. To facilitate egress of organic products, the flask was rotated periodically to mix the viscous molten material in the hot flask. A heat gun was used to move the product along the tube if excessive buildup occurred in one area. The apparatus was then cooled and the product removed from the tube, giving 11.42 g of crude product, identified by GC-MS and powder XRD analysis as a mixture of roughly equal weights of **1** and imidazole (1:3 molar ratio). The mixture was repeatedly extracted with hot toluene and

\*To whom correspondence should be addressed: Tel: +01 303 713 5226; fax +01 303 713 5788; e-mail: david.schubert@borax.com.

**Table 1.** Crystallographic Data and Structure Refinement Parameters for **1**, **1**·0.5H<sub>2</sub>O, and **1**·B(OH)<sub>3</sub>

	<b>1</b>	<b>1</b> ·0.5H <sub>2</sub> O	<b>1</b> ·B(OH) <sub>3</sub>
formula, formula wt	C <sub>9</sub> H <sub>6</sub> N <sub>6</sub> , 198.20	C <sub>18</sub> H <sub>14</sub> N <sub>12</sub> O, 414.41	C <sub>9</sub> H <sub>9</sub> BN <sub>6</sub> O <sub>3</sub> , 260.02
temperature (K)	173(2)	173(2)	173(2)
wavelength (Å)	1.54178	1.54178	1.54178
crystal system	triclinic	triclinic	trigonal
space group	P\bar{1}	P\bar{1}	P\bar{3}
unit cell dimensions			
<i>a</i> (Å)	7.2138(12)	7.5608(3)	10.1186(3)
<i>b</i> (Å)	8.3667(15)	7.5669(5)	10.1186(3)
<i>c</i> (Å)	8.8361(13)	15.8436(8)	6.3488(4)
$\alpha$ (°)	99.826(13)	84.504(3)	90
$\beta$ (°)	113.825(10)	81.269(3)	90
$\gamma$ (°)	110.721(11)	87.038(3)	120
volume (Å <sup>3</sup> ), <i>Z</i>	424.55(12), 2	891.18(8), 2	562.94(4), 2
density (calcd, Mg/m <sup>3</sup> )	1.550	1.544	1.534
absorption coefficient (mm <sup>-1</sup> )	0.872	0.899	0.997
<i>F</i> (000)	204	428	268
crystal size, mm <sup>3</sup>	0.41 × 0.10 × 0.04	0.32 × 0.23 × 0.08	0.25 × 0.17 × 0.12
$\theta$ range for data collection (°)	5.88–66.42	2.83–66.14	5.05–65.87
index ranges	$-8 \leq h \leq 8$ $-9 \leq k \leq 9$ $-10 \leq l \leq 10$	$-8 \leq h \leq 8$ $-8 \leq k \leq 7$ $-18 \leq l \leq 18$	$-11 \leq h \leq 11$ $8 \leq k \leq 11$ $-7 \leq l \leq 7$
reflections collected	4746	7010	3797
independent reflections	1383 [R(int) = 0.0436] ( $\theta = 66.42^\circ$ ) 91.7%	2771 [R(int) = 0.0240] ( $\theta = 66.14^\circ$ ) 89.5%	635 [R(int) = 0.0169] ( $\theta = 65.87^\circ$ ) 97.1%
completeness to theta			
absorption correction	semiempirical from equivalents	semiempirical from equivalents	semiempirical from equivalents
max and min transmission	0.9676 and 0.7163	0.9315 and 0.7618	0.8897 and 0.7886
refinement method	full-matrix least-squares on <i>F</i> <sup>2</sup> 1383/0/161	full-matrix least-squares on <i>F</i> <sup>2</sup> 2771/0/280	full-matrix least-squares on <i>F</i> <sup>2</sup> 635/0/63
data/restraints/parameters	1.092	1.046	1.102
goodness-of-fit on <i>F</i> <sup>2</sup>			
final <i>R</i> indices [ <i>I</i> > 2σ( <i>I</i> )]	<i>R</i> <sub>1</sub> = 0.0551, <i>wR</i> <sub>2</sub> = 0.1697	<i>R</i> <sub>1</sub> = 0.0435, <i>wR</i> <sub>2</sub> = 0.1163	<i>R</i> <sub>1</sub> = 0.0284, <i>wR</i> <sub>2</sub> = 0.0798
<i>R</i> indices (all data)	<i>R</i> <sub>1</sub> = 0.0753, <i>wR</i> <sub>2</sub> = 0.1970	<i>R</i> <sub>1</sub> = 0.0482, <i>wR</i> <sub>2</sub> = 0.1202	<i>R</i> <sub>1</sub> = 0.0298, <i>wR</i> <sub>2</sub> = 0.0810
extinction coefficient	0.007(3)	NA	0.0056(10)
largest diff peak and hole (e Å <sup>-3</sup> )	0.278 and -0.256	0.225 and -0.222	0.145 and -0.157

solvent was removed using a rotovap to give 6.28 g (76% yield) of substantially pure anhydrous **1** identified by <sup>1</sup>H and <sup>13</sup>C NMR, GC-MS, and elemental analysis data [<sup>1</sup>H NMR (300 MHz, C<sub>6</sub>D<sub>6</sub>): δ 7.27 (d, 1 H, <sup>3</sup>J<sub>H-H</sub> ~ 3 Hz), δ 7.81 (d, 1 H, <sup>3</sup>J<sub>HH</sub> ~ 3 Hz); <sup>13</sup>C NMR (75 MHz, C<sub>6</sub>D<sub>6</sub>): δ 111.82 (1 C), 129.22 (1 C), 135.40 (1 C); Anal. Found: C, 54.15; H, 3.01; N, 42.16. Calc. for C<sub>9</sub>H<sub>6</sub>N<sub>6</sub>: C, 54.54; H, 4.44; N, 42.40]. Further purification of **1** was carried out by column chromatography on silica gel using CH<sub>2</sub>Cl<sub>2</sub> solvent, where **1** eluted first followed by a minor amount of **iso-1a** (described below), and last imidazole. The minor **iso-1a** band is associated with fluorescence under a black light, thus assisting in this separation. The powder XRD pattern of product **1** agreed well with that generated from single-crystal data.

**Synthesis of Cyclic Triimidazole-Boric Acid Adduct, **1**·B(OH)<sub>3</sub>.** A solution of **1** (99.1 mg, 0.50 mmol) in 5 mL of hot water was mixed with a solution of boric acid (30.9 mg, 0.50 mmol) in 1 mL of water. The resulting solution was cooled and evaporated to dryness, leaving a quantitative yield of colorless acicular crystals. Powder XRD analysis of this product showed only the pattern agreeing with that simulated from single-crystal data for **1**·B(OH)<sub>3</sub> and did not show the presence of either starting material. Anal. Found: B, 4.16; C, 41.57; H, 3.49; N, 32.32. Calc. for BC<sub>9</sub>H<sub>9</sub>N<sub>6</sub>O<sub>3</sub>: B, 3.69; C, 42.21; H, 3.31; N, 31.86. Crystalline fibers of **1**·B(OH)<sub>3</sub> having sufficient volume for single-crystal X-ray structure determination were prepared by dissolving this adduct in hot water followed by slow cooling and evaporation of water.

**Single-Crystal X-ray Data Collections and Structure Determinations.** X-ray diffraction studies were carried out at the Crystallography Laboratory of Emory University, Atlanta, GA. All structured compounds presented colorless crystals, which were grown by slow evaporation of solvent [methylene chloride for anhydrous **1** and water for **1**·0.5H<sub>2</sub>O and **1**·B(OH)<sub>3</sub>]. Details of crystallographic data collections and refinement parameters are given in Table 1. Hydrogen positions were refined for anhydrous **1**, whereas hydrogen atoms attached to carbon atoms were placed in calculated positions for **1**·0.5H<sub>2</sub>O and **1**·B(OH)<sub>3</sub>. Intermolecular

distances were calculated using Diamond v. 3.2f from Crystal Impact.

## Results and Discussion

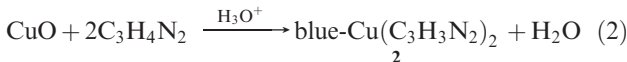
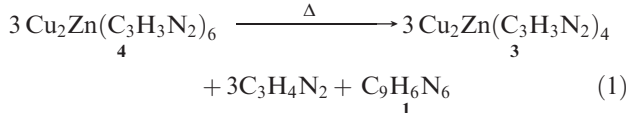
Synthesis of cyclic triimidazole (**1**) by thermolysis of 2-fluoroimidazole was described nearly four decades ago.<sup>3,4</sup> More recently, synthesis of this compound was carried out by photolysis of 2-azoimidazole in 1-butyl-3-methylimidazolium tetrafluoroborate ionic liquid solvent, where 2-fluoroimidazole is an intermediate.<sup>5</sup> In addition, C-substituted derivatives of **1** have also been prepared from C-substituted 2-fluoro- and 2-aryloxy-imidazoles.<sup>6,7</sup> Notably, C-substituted derivatives of triimidazole, including tribenzimidazole, were prepared by oxidation of the parent monomer with copper(II) chloride.<sup>6</sup> Although formation of **1** in up to 56% yield is reported from 2-azoimidazole, this precursor is inconvenient to prepare, and specialized photolysis equipment is required.<sup>5</sup> Herein we describe an alternative method for the facile preparation of multigram quantities of **1** involving thermolysis of the easily prepared copper imidazolate framework solid, Cu(C<sub>3</sub>H<sub>3</sub>N<sub>2</sub>)<sub>2</sub> (**2**).<sup>7</sup> This method provides a simple and inexpensive route to **1**, making it more readily available for further studies.

We previously described the synthesis and crystal structure of the Cu(I)-containing bimetallic imidazolate framework solid, Cu<sub>2</sub>Zn(C<sub>3</sub>H<sub>3</sub>N<sub>2</sub>)<sub>4</sub> (**3**), formed by mild thermolysis of the Cu(II)-containing Cu<sub>2</sub>Zn(C<sub>3</sub>H<sub>3</sub>N<sub>2</sub>)<sub>6</sub> (**4**).<sup>8,9</sup> We reported that formation of **3** was accompanied by generation of **1**, apparently via reductive elimination of the imidazolate ligand and subsequent disproportionation of the imidazole radical to 1-H-imidazole and **1**, in an overall reaction given by eq 1. We also previously described a convenient acid-catalyzed aqueous synthesis of the blue polymorph of the Cu(II) homometallic

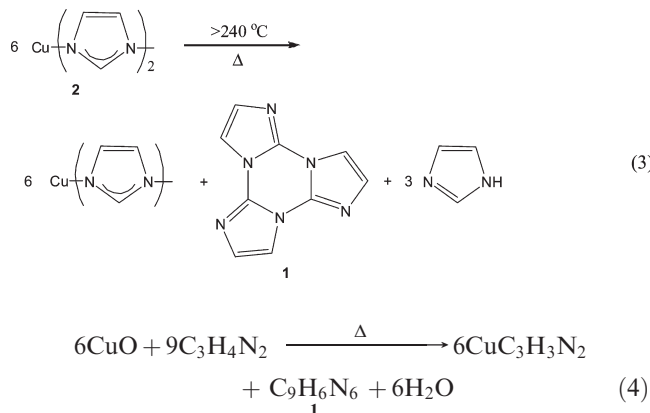
**Table 2.** Bond Lengths [Å] and Angles [°] for Anhydrous Cyclic Triimidazole (**1**)

C(2)–N(3)	1.296(4)	C(14)–H(14)	0.95(3)	N(13)–C(12)–N(11)	113.6(3)
C(2)–N(1)	1.365(4)	C(15)–N(11)	1.385(4)	N(13)–C(12)–N(1)	129.4(3)
C(2)–N(6)	1.397(4)	C(15)–H(15)	0.96(3)	N(11)–C(12)–N(1)	116.9(3)
C(4)–C(5)	1.342(5)	N(3)–C(2)–N(1)	114.3(3)	C(15)–C(14)–N(13)	111.7(3)
C(4)–N(3)	1.401(4)	N(3)–C(2)–N(6)	129.2(3)	C(15)–C(14)–H(14)	125(2)
C(4)–H(4)	0.98(3)	N(1)–C(2)–N(6)	116.5(3)	N(13)–C(14)–H(14)	123(2)
C(5)–N(1)	1.400(4)	C(5)–C(4)–N(3)	112.0(3)	C(14)–C(15)–N(11)	105.4(3)
C(5)–H(5)	0.94(3)	C(5)–C(4)–H(4)	127.3(18)	C(14)–C(15)–H(15)	131(2)
C(7)–N(8)	1.308(3)	N(3)–C(4)–H(4)	120.8(18)	N(11)–C(15)–H(15)	123.3(19)
C(7)–N(6)	1.366(4)	C(4)–C(5)–N(1)	105.3(3)	C(2)–N(1)–C(12)	123.4(2)
C(7)–N(11)	1.384(4)	C(4)–C(5)–H(5)	134(2)	C(2)–N(1)–C(5)	105.3(3)
C(9)–C(10)	1.351(5)	N(1)–C(5)–H(5)	121(2)	C(12)–N(1)–C(5)	131.2(3)
C(9)–N(8)	1.386(4)	N(8)–C(7)–N(6)	113.4(3)	C(2)–N(3)–C(4)	103.1(3)
C(9)–H(9)	0.99(3)	N(8)–C(7)–N(11)	129.2(3)	C(7)–N(6)–C(10)	105.9(3)
C(10)–N(6)	1.390(4)	N(6)–C(7)–N(11)	117.4(3)	C(7)–N(6)–C(2)	123.0(3)
C(10)–H(10)	0.91(3)	C(10)–C(9)–N(8)	112.0(3)	C(10)–N(6)–C(2)	131.1(3)
C(12)–N(13)	1.297(4)	C(10)–C(9)–H(9)	128(2)	C(7)–N(8)–C(9)	103.6(3)
C(12)–N(11)	1.374(4)	N(8)–C(9)–H(9)	120(2)	C(12)–N(11)–C(7)	122.7(3)
C(12)–N(1)	1.388(4)	C(9)–C(10)–N(6)	105.2(3)	C(12)–N(11)–C(15)	105.6(2)
C(14)–C(15)	1.352(4)	C(9)–C(10)–H(10)	132.3(18)	C(7)–N(11)–C(15)	131.6(3)
C(14)–N(13)	1.392(5)	N(6)–C(10)–H(10)	122.4(18)	C(12)–N(13)–C(14)	103.6(3)

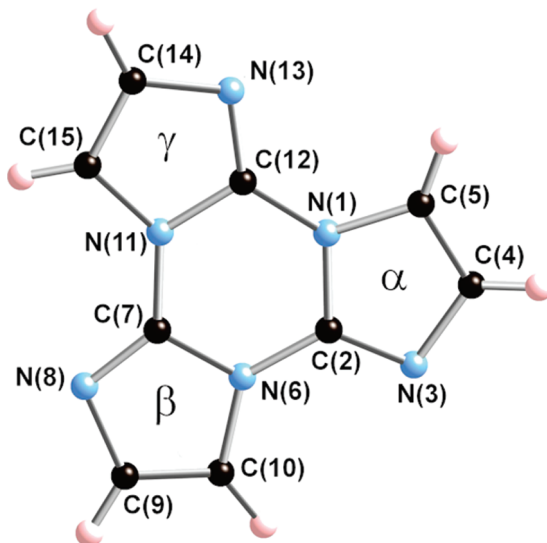
imidazolate framework compound, Cu(C<sub>3</sub>H<sub>3</sub>N<sub>2</sub>)<sub>2</sub> (**2**)<sup>2,10</sup> from inexpensive copper(II) oxide and imidazole, according to eq 2.<sup>11</sup> In a reaction



analogous to that given by eq 1, we found that heating neat **2** above ca. 240 °C results in decomposition with remarkably clean formation of 1-H-imidazole and **1** in approximately equal weights, nominally according to the redox reaction given by eq 3, where **1** is obtained in up to 76% isolated yield. Thus, **1** is easily prepared by this method in two simple steps from relatively inexpensive reagents according to the net reaction given by eq 4.



The organic products of eq 3 are readily separated from the solvent-free reaction system by in situ vacuum sublimation. These products cosublime and are not easily separated by differential sublimation. We found that substantially pure **1** can be separated from the imidazole coproduct by extraction into toluene, where this solvent can be recycled indefinitely. Further purification of **1** can be accomplished by column chromatography on silica gel.

**Figure 1.** Atoms labels used for **1** molecules in crystal structures.

During thermolysis of **2** under a vacuum in the 200–330 °C temperature range, the copper-containing residue melts to form a viscous mass. Upon cooling, a porous reddish-brown hard sintered mass is obtained. Analysis of this material by powder XRD indicates that it is primarily amorphous with no evidence for the presence of crystalline Cu(I) imidazolate, which has been previously described;<sup>12</sup> however, it does show the presence of some metallic copper. Thus, the thermolysis reaction is clearly more complex than suggested by eq 3, with some fraction of the copper being fully reduced to the elemental state.

Equation 3 presumably involves disproportionation of the imidazole radical formed by 1-electron reductive elimination from **2**. Compound **1** apparently results from radical attack at the 2-position of imidazole ring. A significant minor isomer (*iso-1a*) is observed by GC-MS analysis of the product. Although we were unable to isolate a sufficient quantity of this isomer for characterization, we propose that it arises from a competing 4,5-attack to produce a product analogous to **1** with nitrogen atoms in different positions in one of the imidazole rings. Multiple 4,5-attack should result in additional isomers of this kind. Indeed, careful examination of

GC-MS data reveals the presence of trace amounts of these additional isomers, having the same mass as **1** with different GC retention times. In addition, trace amounts of tetrameric and pentameric products were also detected, apparently arising from radical attack on trimeric **1**. It can be stressed that thermolysis of **2** is remarkably clean, and most of these byproducts are observed in trace amounts. Only one isomer (**iso-1a**) is observed as a significant portion of the total product. It was found that this isomer is not removed from **1** during extraction with toluene, but can be removed chromatographically by passing the initially extracted product through a silica gel column using methylene chloride solvent, thus providing high purity **1**. However, the initial toluene extract was generally found to be substantially pure reagent grade **1** (> 97%).

Takeuchi et al. reported characterization data for **1** and its C-substituted derivatives, including NMR and UV spectra.<sup>4</sup> They observed that **1** is a weak base that is protonated only by very strong acids and measured the stability of its monohydrochloride salt ( $pK_{app} = 1.5$ ,  $pK = 1.0$ ). Isotopic exchange studies also showed that the hydrogen atoms in **1** undergo exchange for deuterium in the presence of NaOD in  $\text{CD}_3\text{OD}/\text{D}_2\text{O}$  solvent, with the hydrogen atoms on the carbon atoms closest to the central ring nitrogens, labeled H(5), H(10), and H(15) in crystal structures herein, showing much faster exchange than the other hydrogen positions. We observed that **1** readily undergoes electrophilic substitution in the presence of bromine or iodine.

**Structure of Cyclic Triimidazole, 1.** The structure of **1** was determined by single-crystal X-ray diffraction. As expected, this structure is consistent with an 18-electron aromatic system. However, the structure deviates from anticipated idealized  $D_{3h}$  symmetry. Selected bond distances and angles are listed in Table 2 with atom labeling used for structures of **1** molecules presented herein shown in Figure 1.

The **1** molecule in anhydrous **1** is slightly distorted from planarity. The central six-membered ring is nearly planar, with atoms in this ring exhibiting a maximum displacement from the average central ring plane of 0.018(4) Å, but the three imidazole rings are crystallographically nonequivalent and tilted somewhat from the central ring plane. The average planes of the imidazole rings present angles to the average plane of the central six-membered ring of 1.7(2), 1.0(2), and 2.3(2)°, producing a slightly twisted molecule.

The nitrogen atoms in the central six-membered ring in anhydrous **1** display planar geometries. This ring exhibits alternating shorter and longer C–N bond lengths averaging 1.379(2) Å. The central ring imidazole C–N bonds are shorter, averaging 1.368(3) Å, whereas the nonimidazole C–N bonds are longer, averaging 1.390(3) Å. These bonds are longer than typically found in six-membered N-containing aromatic rings [mean = 1.336(14) Å] but shorter than in N-containing aliphatic rings [e.g., piperidine C–N, 1.473(13) Å].<sup>13</sup> The central ring C–N distances in **1** are closer to those found in compounds containing  $\text{sp}^2$ -hybridized planar nitrogen bound to aromatic ring carbon atoms [1.370(16) Å].<sup>13</sup> Bond angles in this central ring result in a geometry that differs significantly from an idealized hexagon, but not as much as in s-triazine.<sup>14</sup> Average C–N–C and N–C–N bond angles in the central ring are 123.0(2)° and 116.0(4)°, respectively, a difference of 6.0(4)° compared with 13.6° for s-triazine. The C–N bond distances are shortened compared to those in aliphatic amines but are longer than those in s-triazine, which are 1.338 Å for the 150 K structure.<sup>14</sup>

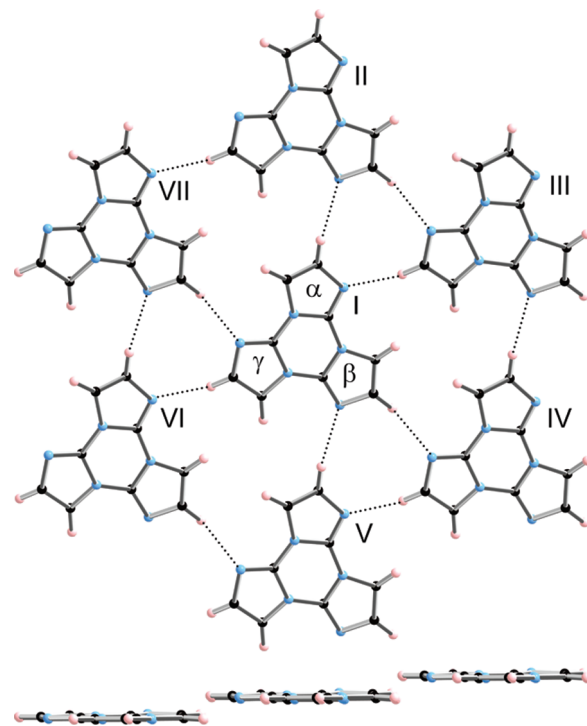


**Figure 2.** Arbitrarily assigned central molecule **I** surrounded by six nearest neighbor molecules (**II**–**VII**) in approximate sheets with nonequivalent imidazole rings labeled  $\alpha$ ,  $\beta$ , and  $\gamma$ . A side view of the same array rotated 90 °C is shown at the bottom.

Molecules of **1** may associate by very weak hydrogen bonding. Each **1** molecule is surrounded by eight nearby **1** molecules involving six close C–H···N approaches, as shown in Figure 2. Labeling the three nonequivalent imidazole rings in **I** as  $\alpha$ ,  $\beta$ , and  $\gamma$ , a C–H group of the  $\alpha$  imidazole ring of an arbitrarily assigned central molecule exhibits a close C–H···N approach with the  $\beta$  ring of an adjacent molecule, labeled **II** in Figure 2 [C(4)···N(8), 3.504(4) Å]. A symmetrically equivalent approach exists between a central molecule nitrogen atom and a C–H group of opposite adjacent molecule **V**. The nitrogen atom of the  $\alpha$  imidazole ring of **I** exhibits a close N···H–C approach with the  $\gamma$  ring of **III** with a symmetrically equivalent  $\gamma$ – $\alpha$  approach with **VI** [N(3)···C(14), 3.518(5) Å]. The nitrogen atom of the  $\gamma$  ring of **I** also shows a close approach with the  $\beta$  ring of **VII** [N(13)···C(9), 3.447(6) Å], with a symmetrically equivalent approach with **IV**.

The central molecule **I** forms planar rows with molecules **II** and **V**, as seen in the 90° rotated view at the bottom of Figure 2. Molecules **III** and **IV** form a similar planar row, which is parallel and located 0.764(2) Å from the average plane containing **I**, **II**, and **V**, whereas molecules **VI** and **VII** also occupy a planar row, which is parallel to the planes of the other molecules pictured in Figure 2 and located –0.764(2) Å from the plane containing **I**, **II**, and **V**. Approximate sheets, such as those containing **I**–**VII**, are created by parallel planar rows of molecules offset from one another by 0.764(2) Å and exhibiting close approaches as described above. Molecules in each sheet have the same orientation.

As shown in Figure 3, **1** molecules stack in an alternating **AB** fashion with every other molecule rotated 180° about an axis normal to their average molecular planes. Molecules in these stacks are positioned in such a way as to provide close approach between relatively electron-rich and electron-poor

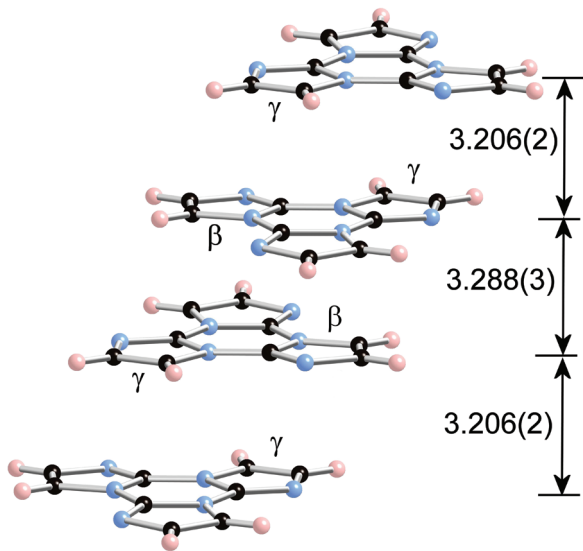


**Figure 3.** Columns of **1** molecules exhibiting **AB** stacking arrangement with distances between molecular planes given in Å and labels on  $\beta$  and  $\gamma$  rings involved in greatest overlap with the central rings of stack neighbors shown.

heteroannular rings of adjacent molecules in the stack, with alternating distances between average molecular planes of 3.204(9) and 3.290(10) Å, as shown in Figure 4. The central six-membered ring of each **1** molecule approaches the  $\alpha$  and  $\beta$  imidazole rings of opposite neighboring molecules, whereas the  $\gamma$  imidazole rings are oriented away from adjacent molecules in the stacks. The average plane of the  $\gamma$  imidazole ring also displays the largest deviation from the average plane of the central ring [2.3(2) $^\circ$ ]. Acknowledging that the subject of  $\pi-\pi$  bonding is controversial, we propose that the slight distortion of the **1** molecule from ideally  $D_{3h}$  symmetry may result from intermolecular stacking interactions.<sup>15,16</sup>

**Structure of Cyclic Triimidazole Hemihydrate, **1**·0.5H<sub>2</sub>O.** Slow evaporation of an aqueous solution of sparingly water-soluble **1** results in formation of the crystalline hemihydrate, **1**·0.5H<sub>2</sub>O, which forms as fragile blocky crystals that slowly lose water in dry air converting to anhydrous microcrystalline **1**. The structure of **1**·0.5H<sub>2</sub>O was determined by single-crystal X-ray diffraction. The asymmetric unit contains two crystallographically independent **1** molecules and one H-bonded water molecule, providing additional structural data for this heteroannular system. Interatomic distances and angles for **1**·0.5H<sub>2</sub>O are listed in Table 3.

The two crystallographically independent **1** molecules in **1**·0.5H<sub>2</sub>O are labeled **1A** and **1B**. Both molecules deviate slightly from ideal  $D_{3h}$  symmetry and exhibit small distortions from planarity. Their central six-membered rings are nearly planar with atoms in these rings showing maximum displacements of 0.009(2) Å for C7A in **1A** and 0.030(3) Å for C12B in **1B**. The nitrogen atoms in both central rings are planar. The average planes of the imidazole rings deviate from coplanarity with the average planes of the central six-membered rings by 0.85(7), 1.07(6), and 0.63(7) $^\circ$  for **1A** and 2.35(7), 2.73(7), and 2.20(7) $^\circ$  for **1B**. Thus, **1B** shows more distortion from ideal  $D_{3h}$  symmetry than **1A**. Bond distances and angles in **1A** and **1B** are similar to one another and also similar to those seen in anhydrous **1**.

Each **1A** molecule is surrounded by seven **1** molecules and one water molecule. Two nearby molecules are **1A** stacking neighbors, lying parallel above and below the plane of the

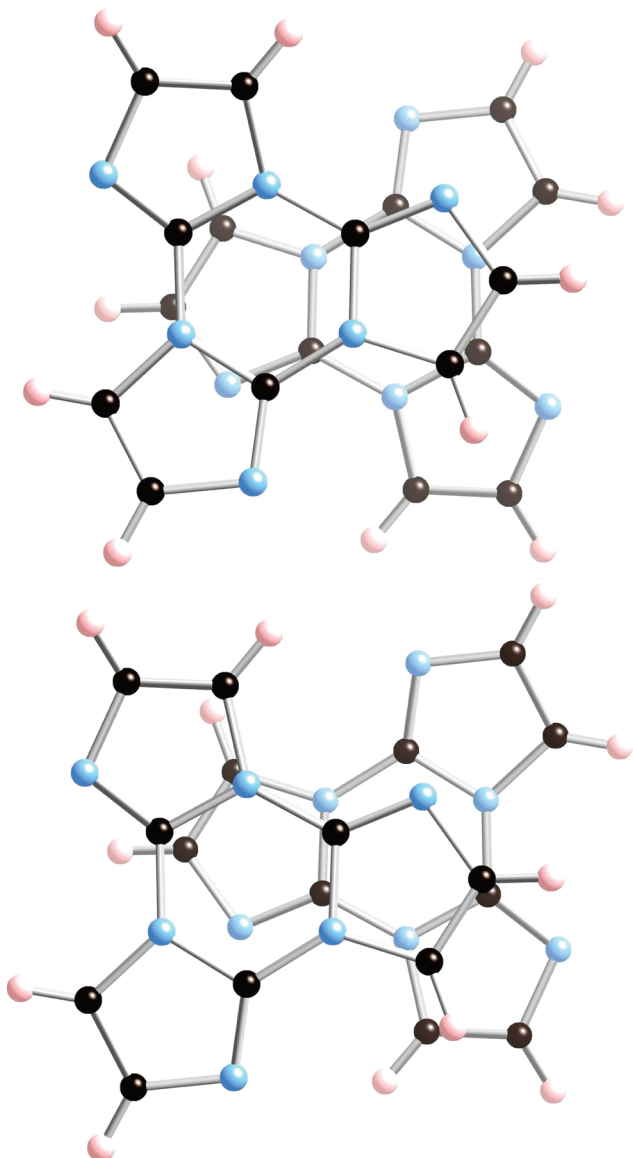


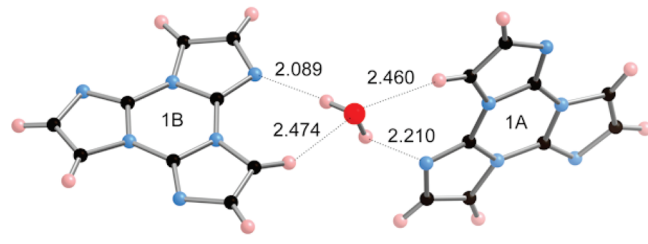
**Figure 4.** View of molecular overlaps in **AB** stacks of **1** molecules. Top:  $\beta$ -imidazole-to-central ring overlaps. Bottom:  $\alpha$ -imidazole-to-central ring overlaps.

molecule, as described below. Two **1A** and three **1B** molecules also lie nearby. Adjacent **1A** molecules form coplanar rows with the central **1A** molecule wherein each molecule is rotated 180° from its nearest row neighbors. The C–H groups of these coplanar **1A** molecules approach the nitrogen atoms of adjacent molecules with C···N distances of 3.289(3) Å [C(4)–N(3)] and 3.361(3) Å [C(15)–N(8)]. In addition, a water molecule donates a O–H···N H-bond [O···N(13A), 3.097(3) Å] and also forms a close C–H···O approach [C(5A)···O, 3.299(3) Å].

Each **1B** molecule is surrounded by ten **1** and two water molecules. Two nearby **1** molecules are **1B** stacking neighbors. Like **1A**, two adjacent **1B** molecules are coplanar and form **1B** rows with each molecule rotated 180° from its nearest row neighbors. Unlike **1A**, these rows contain no C–H···N approaches less than 3.799(4) Å. An additional six **1A** molecules lie nearby. A water molecule donates a O–H···N H-bond [O···N(13B), 2.968(3) Å] and also forms a close C–H···O approach [C(5B)···O, 3.301(3) Å]. A second water molecule lies nearby and forms another

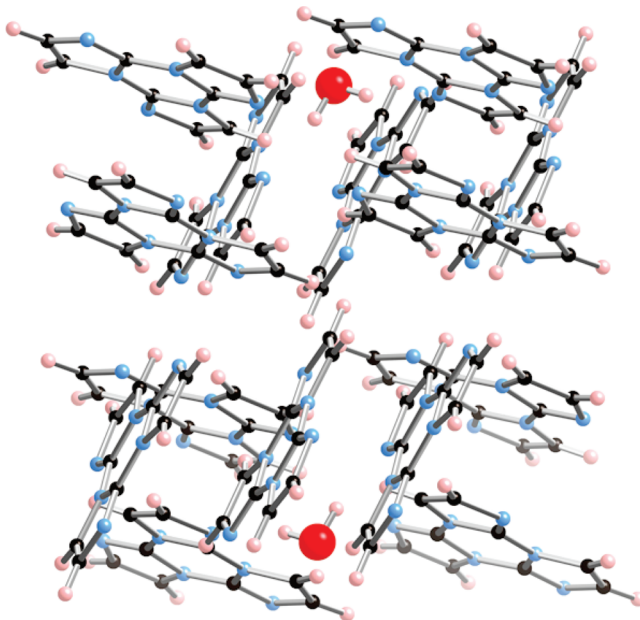
**Table 3.** Bond lengths ( $\text{\AA}$ ) and Angles ( $^\circ$ ) for **1**· $0.5\text{H}_2\text{O}$ 

C(2A)–N(3A)	1.295(3)	C(14B)–N(13B)	1.390(3)	N(8B)–C(7B)–N(11B)	129.5(2)
C(2A)–N(1A)	1.370(2)	C(14B)–H(14B)	0.9500	N(6B)–C(7B)–N(11B)	116.82(17)
C(2A)–N(6A)	1.389(3)	C(15B)–N(11B)	1.397(3)	C(10B)–C(9B)–N(8B)	112.7(2)
C(4A)–C(5A)	1.352(3)	C(15B)–H(15B)	0.9500	C(10B)–C(9B)–H(9B)	123.6
C(4A)–N(3A)	1.392(3)	O(1W)–H(1W)	0.9074	N(8B)–C(9B)–H(9B)	123.6
C(4A)–H(4A)	0.9500	O(1W)–H(2W)	0.9899	C(9B)–C(10B)–N(6B)	104.7(2)
C(5A)–N(1A)	1.395(3)	N(3A)–C(2A)–N(1A)	113.88(18)	C(9B)–C(10B)–H(10B)	127.7
C(5A)–H(5A)	0.9500	N(3A)–C(2A)–N(6A)	128.97(18)	N(6B)–C(10B)–H(10B)	127.7
C(7A)–N(8A)	1.309(3)	N(1A)–C(2A)–N(6A)	117.16(17)	N(13B)–C(12B)–N(11B)	113.81(18)
C(7A)–N(6A)	1.363(3)	C(5A)–C(4A)–N(3A)	112.31(19)	N(13B)–C(12B)–N(1B)	128.89(18)
C(7A)–N(11A)	1.378(3)	C(5A)–C(4A)–H(4A)	123.8	N(11B)–C(12B)–N(1B)	117.29(18)
C(9A)–C(10A)	1.343(3)	N(3A)–C(4A)–H(4A)	123.8	C(15B)–C(14B)–N(13B)	112.7(2)
C(9A)–N(8A)	1.395(3)	C(4A)–C(5A)–N(1A)	104.67(18)	C(15B)–C(14B)–H(14B)	123.7
C(9A)–H(9A)	0.9500	C(4A)–C(5A)–H(5A)	127.7	N(13B)–C(14B)–H(14B)	123.7
C(10A)–N(6A)	1.397(3)	N(1A)–C(5A)–H(5A)	127.7	C(14B)–C(15B)–N(11B)	104.91(19)
C(10A)–H(10A)	0.9500	N(8A)–C(7A)–N(6A)	113.32(18)	C(14B)–C(15B)–N(11B)	104.91(19)
C(12A)–N(13A)	1.303(2)	N(8A)–C(7A)–N(11A)	129.23(19)	C(14B)–C(15B)–H(15B)	127.5
C(12A)–N(11A)	1.365(3)	N(6A)–C(7A)–N(11A)	117.45(17)	N(11B)–C(15B)–H(15B)	127.5
C(12A)–N(1A)	1.380(3)	C(10A)–C(9A)–N(8A)	112.22(19)	C(2A)–N(1A)–C(12A)	122.46(17)
C(14A)–C(15A)	1.346(3)	C(10A)–C(9A)–H(9A)	123.9	C(2A)–N(1A)–C(5A)	105.75(16)
C(14A)–N(13A)	1.393(3)	N(8A)–C(9A)–H(9A)	123.9	C(12A)–N(1A)–C(5A)	131.79(17)
C(14A)–H(14A)	0.9500	C(9A)–C(10A)–N(6A)	104.98(19)	C(2A)–N(3A)–C(4A)	103.39(17)
C(15A)–N(11A)	1.392(3)	C(9A)–C(10A)–H(10A)	127.5	C(7A)–N(6A)–C(2A)	122.60(17)
C(15A)–H(15A)	0.9500	N(6A)–C(10A)–H(10A)	127.5	C(7A)–N(6A)–C(10A)	106.12(17)
C(2B)–N(3B)	1.299(3)	N(13A)–C(12A)–N(11A)	113.52(18)	C(2A)–N(6A)–C(10A)	131.27(19)
C(2B)–N(1B)	1.363(3)	N(13A)–C(12A)–N(1A)	128.92(18)	C(7A)–N(8A)–C(9A)	103.35(18)
C(2B)–N(6B)	1.386(3)	N(11A)–C(12A)–N(1A)	117.55(17)	C(12A)–N(11A)–C(7A)	122.76(17)
C(4B)–C(5B)	1.346(3)	C(15A)–C(14A)–N(13A)	112.24(18)	C(12A)–N(11A)–C(15A)	106.08(17)
C(4B)–N(3B)	1.391(3)	C(15A)–C(14A)–H(14A)	123.9	C(7A)–N(11A)–C(15A)	131.16(18)
C(4B)–H(4B)	0.9500	N(13A)–C(14A)–H(14A)	123.9	C(12A)–N(13A)–C(14A)	103.28(17)
C(5B)–N(1B)	1.399(3)	C(14A)–C(15A)–N(11A)	104.87(18)	C(2B)–N(1B)–C(12B)	122.86(17)
C(5B)–H(5B)	0.9500	C(14A)–C(15A)–H(15A)	127.6	C(2B)–N(1B)–C(5B)	105.37(16)
C(7B)–N(8B)	1.297(3)	N(11A)–C(15A)–H(15A)	127.6	C(12B)–N(1B)–C(5B)	131.76(17)
C(7B)–N(6B)	1.375(3)	N(3B)–C(2B)–N(1B)	114.29(17)	C(2B)–N(3B)–C(4B)	103.02(17)
C(7B)–N(11B)	1.389(3)	N(3B)–C(2B)–N(6B)	128.22(19)	C(7B)–N(6B)–C(2B)	122.56(18)
C(9B)–C(10B)	1.347(4)	N(1B)–C(2B)–N(6B)	117.44(17)	C(7B)–N(6B)–C(10B)	105.89(18)
C(9B)–N(8B)	1.392(3)	C(5B)–C(4B)–N(3B)	112.42(18)	C(2B)–N(6B)–C(10B)	131.41(19)
C(9B)–H(9B)	0.9500	C(5B)–C(4B)–H(4B)	123.8	C(7B)–N(8B)–C(9B)	103.0(2)
C(10B)–N(6B)	1.389(3)	C(4B)–C(5B)–N(1B)	104.89(17)	C(12B)–N(11B)–C(7B)	122.84(18)
C(10B)–H(10B)	0.9500	N(3B)–C(4B)–H(4B)	123.8	C(12B)–N(11B)–C(15B)	105.56(18)
C(12B)–N(13B)	1.303(3)	C(4B)–C(5B)–H(5B)	127.6	C(7B)–N(11B)–C(15B)	131.58(19)
C(12B)–N(11B)	1.367(3)	N(1B)–C(5B)–H(5B)	127.6	C(12B)–N(13B)–C(14B)	103.05(18)
C(12B)–N(1B)	1.381(3)	N(8B)–C(7B)–N(6B)	113.7(2)	H(1W)–O(1W)–H(2W)	100.2
C(14B)–C(15B)	1.340(3)				

**Figure 5.** Interaction between water and **1** molecules in **1**· $0.5\text{H}_2\text{O}$ , showing distances from H atoms to N and O atoms in  $\text{\AA}$ .

close C–H $\cdots$ O, 3.354(3)  $\text{\AA}$ . Water molecules link **1A** and **1B** molecules with pairs of O–H $\cdots$ N and possible weak C–H $\cdots$ O interactions with distances given above, as shown in Figure 5.

Similar to the supramolecular structure of anhydrous **1**, one-dimensional rows of **1A** and **1B** molecules stack in an **AB** fashion with stacked molecules rotated 180° about the normals to the average planes of adjacent molecules within the stacks. Also like anhydrous **1**, molecules within these stacks are oriented in such a way as to permit close approach between relatively electron-rich and electron-poor molecular regions with stacks presenting alternating shorter and longer distances between the average planes of the molecules in each stack. The interplanar distances in these stacks are 3.260(4)

**Figure 6.** Supramolecular structure of **1**· $0.5\text{H}_2\text{O}$ .

and 3.282(4)  $\text{\AA}$  for **1A** and 3.311(2) and 3.334(2)  $\text{\AA}$  for **1B**. Notably, the longest stacking distance is associated with the

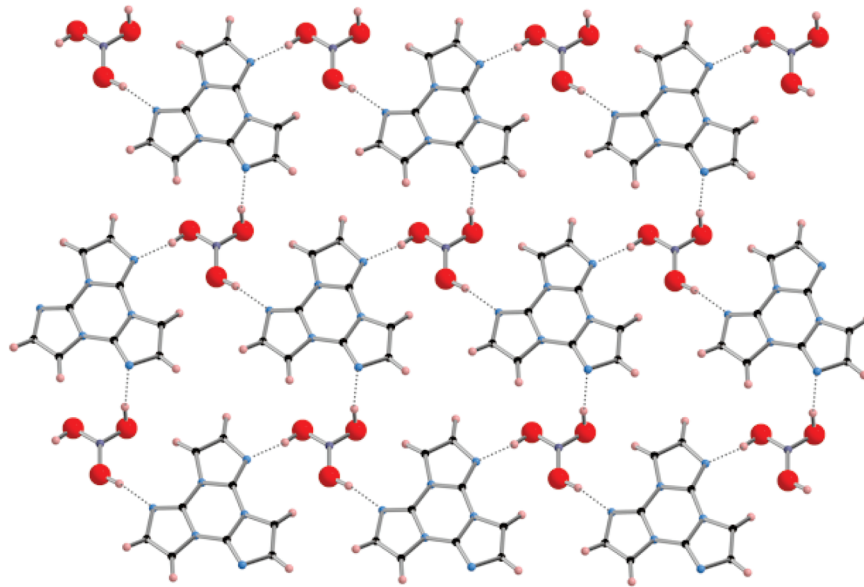


**Figure 7.** Section of H-bonded sheets in  $\mathbf{1} \cdot \text{B(OH)}_3$ .

**Table 4. Bond Lengths [Å] and Angles [°] for Cyclic Triimidazole-Boric Acid Adduct,  $\mathbf{1} \cdot \text{B(OH)}_3^a$**

B(1)–O(1)#1	1.3605(9)	O(1)–H(1O)	0.95(2)	N(3)–C(2)–N(1)#3	129.30(11)
B(1)–O(1)	1.3605(9)	O(1)#1–B(1)–O(1)	120.000(1)	C(2)–N(3)–C(4)	103.54(11)
B(1)–O(2)#2	1.3605(9)	O(1)–B(1)–O(1)#2	119.999(1)	C(5)–C(4)–N(3)	112.15(11)
N(1)–C(2)#4	1.3883(15)	O(1)#1–B(1)–O(1)#2	120.001(1)	N(3)–C(4)–H(2)	123.9
C(2)–N(1)	1.3685(15)	B(1)–O(1)–H(1O)	115.7(11)	N(3)–C(4)–H(2)	123.9
C(2)–N(1)#3	1.3883(15)	C(2)–N(1)–C(2)#4	122.75(10)	C(5)–C(4)–H(2)	123.9
C(2)–N(3)	1.2973(15)	C(2)–N(1)–C(5)	106.15(10)	C(4)–C(5)–N(1)	104.72(10)
C(4)–N(3)	1.3921(16)	C(2)#4–N(1)–C(5)	131.11(10)	N(1)–C(5)–H(1)	127.6
C(5)–C(4)	1.3505(18)	N(3)–C(2)–N(1)	113.44(11)		
C(5)–N(1)	1.3898(14)	N(1)–C(2)–N(1)#3	117.25(10)		

<sup>a</sup> Symmetry transformations used to generate equivalent atoms: #1  $-x + y - 1, -x, z$ , #2  $-y, x - y + 1, z$ , #3  $-x + y, -x + 1, z$ , #4  $-y + 1, x - y + 1, z$ .

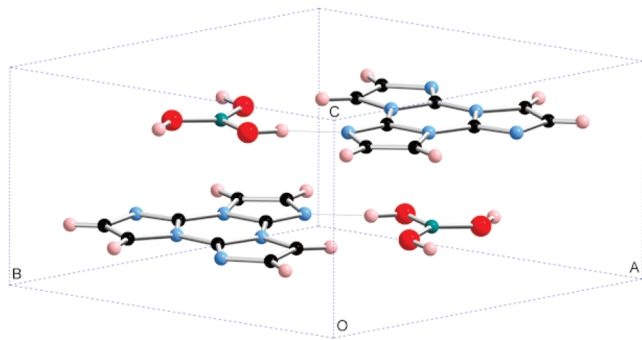


**Figure 8.** View of unit cell in  $\mathbf{1} \cdot \text{B(OH)}_3$ .

poorest molecular overlap between **1B** molecules, involving only imidazole rings and not the central ring. Stacks of **1A** and **1B** molecules form the crystallographic angle  $\alpha$  with respect to one another, as shown in Figure 6.

**Cyclic Triimidazole-Boric Acid Adduct,  $\mathbf{1} \cdot \text{B(OH)}_3$ .** We observed that **1** forms adducts with a range of H-bond donor molecules, including cyanuric acid, 1,3,5-trihydroxybenzene (phlorogucinol), and 1- and 2-naphthol. Although orthoboric acid is known to form H-bonded adducts with certain organic molecules, such as the 1:2 adduct with melamine,  $\text{C}_3\text{N}_6\text{H}_6 \cdot 2\text{B(OH)}_3$ , this is a relatively unexplored area.<sup>17</sup> Mixing aqueous solutions of **1** and boric acid results in the quantitative formation of a 1:1 adduct. Microscopic examination of this product reveals long fibers when very

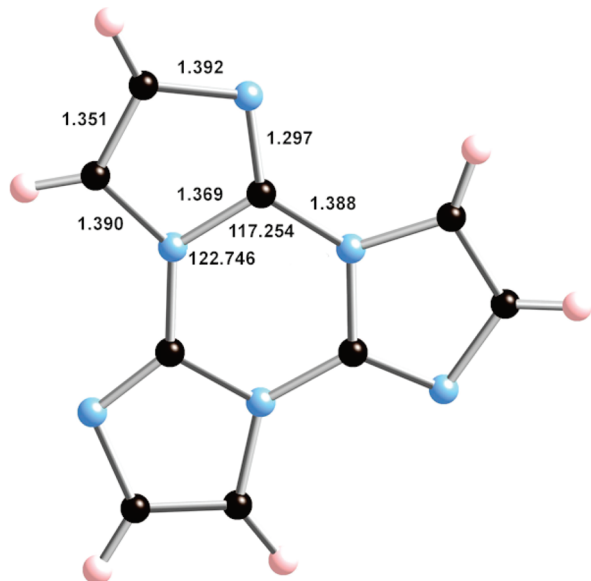


**Figure 9.** Distances and central ring angles for the 3-fold symmetric **1** molecule in  $\mathbf{1} \cdot \text{B(OH)}_3$ .

pure **1** is used and needle-shaped crystals when less pure **1** is used.

The crystal structure of  $\mathbf{1} \cdot \text{B(OH)}_3$  reveals planar sheets of H-bonded **1** and  $\text{B(OH)}_3$  molecules, as shown in Figure 7. Bond distances and angles for  $\mathbf{1} \cdot \text{B(OH)}_3$  are listed in Table 4.

The structure of **1**·B(OH)<sub>3</sub> is integrated by a network of O—H···N H-bonds with O···N donor–acceptor distances of 2.778(2) Å [O—H, 0.95(2) Å; H···N, 1.84(2) Å, O—H—N 167(2)°]. In addition, a close approach occurs between a C—H group and a boric acid oxygen atom [C(5)···O, 3.222(2) Å; C—H—O 168.9(1)°]. The H-bonded sheets in **1**·B(OH)<sub>3</sub> exhibit an **AB** stacking arrangement with interplanar separations of 3.175(4) Å with boric acid boron atoms positioned above and below the centroids of **1** molecules, as shown in the unit cell diagram, Figure 8. The boric acid boron atoms lie 3.175(4) Å above and below the centroid of each **1** molecule along axes normal to the sheets and passing through the centroids. The boric acid molecule in **1**·B(OH)<sub>3</sub> is similar to that in pure boric acid. The molecule is planar with B—O distances of 1.3605(9) Å, which is similar to that found in the commonly cited crystal structure for this substance, 1.368 Å.<sup>18</sup> It can be noted that pure boric acid also presents a sheet structure integrated by H-bonds with an interplanar distance of 3.05 Å, which is shorter than in **1**·B(OH)<sub>3</sub> [3.175(4) Å].<sup>18</sup> For comparison, both of these compounds exhibit substantially shorter interplanar separations than found in conventional **AB** graphite, 3.35 Å.<sup>19</sup> In contrast to **1**·B(OH)<sub>3</sub>, the room temperature structure of boric acid exhibits a disorder sheet stacking arrangement, implying that stronger intersheet interactions exist in the **1** adduct.

The **1** molecule in **1**·B(OH)<sub>3</sub> does not stack with other **1** molecules as in anhydrous **1** and **1**·0·5H<sub>2</sub>O. Instead, it lies in a symmetrical environment and is crystallographically required to exhibit ideal *D*<sub>3</sub>*h* symmetry. Interatomic distances and central ring angles for this molecule are shown in Figure 9.

### Conclusions

Molecules having the ability to organize supramolecular systems with well-defined symmetries provide valuable tools for crystal design and engineering. The ability of cyclic triimidazole to act as a 3-fold hydrogen bond acceptor suggests its usefulness in supramolecular design and templating. The 1:1 adduct with boric acid provides an example of a highly organized system involving this molecule. The structures of anhydrous **1** and **1**·0·5H<sub>2</sub>O both exhibit **1** molecules that are significantly distorted from idealized geometry. These distortions appear to result from intermolecular stacking interactions. Only the boric acid adduct, **1**·B(OH)<sub>3</sub>, presents this molecule in idealized *D*<sub>3</sub>*h* symmetry.

Facile synthesis of **1** via thermolysis of the easily prepared copper imidazolate framework solid, **2**, provides a convenient route to this material from relatively inexpensive copper(II) oxide and imidazole, making it more readily available for further study. Moreover, this synthesis suggests the possibility

of using metal organic frameworks as synthetic intermediates for other useful organic molecules.

**Acknowledgment.** The principal author wishes to thank Prof. Piotr Kaszynski of Vanderbilt University, Prof. Shih-Yuan Liu of the University of Oregon, and Dr. Donald Camaioni of the Pacific Northwest National Laboratory (PNNL) for helpful discussions and Dr. John Linehan of PNNL for high field NMR spectra.

**Supporting Information Available:** Crystallographic information files. This information is also available free of charge via the Internet at <http://pubs.acs.org/>. Crystallographic data for the crystal structures reported in this paper have been deposited with the Cambridge Crystallographic Database (CCDC Nos. 804409–804411). This material can be obtained free of charge at [www.ccdc.cam.ac.uk/conts/retrieving.html](http://www.ccdc.cam.ac.uk/conts/retrieving.html) (or from the CCDC, 12 Union Road, Cambridge CB2 1EZ, UK; fax +44 1223 336033; e-mail: deposit@ccdc.cam.ac.uk).

### References

- (1) Simard, M.; Su, D.; Wuest, J. D. *J. Am. Chem. Soc.* **1991**, *113*, 4696–4698.
- (2) Masciocchi, N.; Bruni, S.; Cariati, E.; Cariati, F.; Galli, S.; Sironi, A. *Inorg. Chem.* **2001**, *40*, 5897–5905.
- (3) Kirk, K. I.; Nagai, W.; Cohen, L. A. *J. Am. Chem. Soc.* **1973**, *95*, 8389–8391.
- (4) Takeuchi, Y.; Kirk, K. L.; Cohen, L. A. *J. Org. Chem.* **1979**, *44*, 4243–4246.
- (5) Heredia-Moya, J.; Kirk, K. L. *J. Fluorine Chem.* **2007**, *128*, 674–678.
- (6) Ishida, S.; Fukushima, Y.; Sekiguchi, S.; Matsui, K. *Bull. Chem. Soc. Jpn.* **1975**, *48*, 956–959.
- (7) Bhattacharya, R.; Ray, S.; Ray, J.; Ghosh, A. *Central Eur. Sci. J. Chem.* **2003**, *4*, 427–440.
- (8) Schubert, D. M.; Visi, M. Z.; Knobler, C. B. *Main Group Chem.* **2008**, *7*, 311–322.
- (9) Schubert, D. M.; Natan, D. T.; Knobler, C. B. *Inorg. Chim. Acta* **2009**, *362*, 4832–4836.
- (10) Bauman, J. E.; Wang, J. C. *Inorg. Chem.* **1964**, *3*, 368–373.
- (11) Schubert, D. M. Patent Appl. WO2007087434(A2), 2007.
- (12) Tian, Y.-Q.; Xu, H.-J.; Weng, L.-H.; Chen, Z-X; Zhao, D.-Y.; You, X.-Z. *Eur. J. Inorg. Chem.* **2004**, *9*, 1813–1816.
- (13) Allen, F. H.; Kennard, O.; Watson, D. G.; Brammer, L.; Orpen, A. G.; Taylor, R. J. *Chem. Soc. Perkin Trans. II* **1987**, S1–S19.
- (14) Smith, H.; Rae, A. I. M. *J. Phys. C: Solid State Phys.* **1978**, *11*, 1761–1770.
- (15) Grimme, S. *Angew. Chem.* **2008**, *47*, 3430–3434.
- (16) Malathysony, S. M.; PonnuSwamy, M. N. *Cryst. Growth Des.* **2006**, *6*, 736–742.
- (17) Roy, A.; Choudhury, A.; Rao, C. N. R. *J. Mol. Struct.* **2002**, *613*, 61–66.
- (18) Gajihede, M.; Larsen, S.; Retstrup, S. *Acta Crystallogr.* **1986**, *B42*, 545–552.
- (19) Girifalco, L. A.; Lad, R. A. *J. Chem. Phys.* **1956**, *25*, 693–697.